THERMAL STABILITY AND ELECTRICAL PROPERTIES OF DBSA DOPED CETYLTRIMETHYL AMMONIUM BROMIDE FACILITATED PANI@GN NANOCOMPOSITES

Mahfoozurrahman Khan[1], Faiz Mohammad[2*]
[1]Ph.D Research Scholar, Department of Applied Chemistry
Aligarh Muslim University Aligarh, India
[2]Professor, Department of Applied Chemistry
Aligarh Muslim University Aligarh, India
[*]Corresponding author's E-mail: faizmohammad54@rediffmail.com

ABSTRACT

Using innovative approach, the electrically conductive dodecylbenzenesulfonic acid (DBSA) doped polyaniline@graphene (Pani@GN) nanocomposites containing different amounts of graphene were prepared by *in-situ* oxidative polymerization by using $K_2S_2O_8$ as an oxidant. Cetyltrimethylammonium bromide (CTAB) was added into the reaction mixture for uniform and homogeneous distribution of components in the Pani@GN:DBSA nanocomposites. Thus prepared nanocomposites were characterized by Fourier Transform Infra-red Spectroscopy (FTIR), X-Ray Diffraction (XRD), Field Emission Scanning Electron Microscopy (FESEM), Thermogravimetric Analysis (TGA) and Differential Thermal Analysis (DTA). CTAB and DBSA played the role of surfactant for the enhanced uniform dispersion of graphene sheets within the polymer matrix besides DBSA acted as dopant also. Incorporation of graphene nanofiller improved electrical properties and thermal stability of nanocomosites. The FTIR supports the presence of π–π interactions between Pani and GN due to the formation of charge-transfer nanocomposites. Pani@GN:DBSA nanocomposites showed higher thermal stability than the Pani: DBSA. Stability in terms of DC electrical conductivity retention was studied by isothermal and cyclic ageing techniques and was observed to be better than that of Pani under ambient environmental conditions.

Keywords: DBSA doped Pani@GN nanocomposites, *in-situ* polymerization, electron microscopy, thermal stability, electrical properties, isothermal and cyclic ageing techniques.

1. INTRODUCTION

In the recent years, graphene has gained attraction in replacing some of the currently used materials in leading technologies. Graphene is a marvellous material and has two-dimensional nanoscaled structure, single-atom thick and having two dimensional sp^2-hybrized carbon atoms. It has many outstanding properties such as high electrical conductivity and thermal stability, superior mechanical properties, high specific area and low fabrication cost. Hence, graphene is considered as one of the best candidates for electrode materials due to its electronic transport properties and conductivity. It has been predicted to hold great promise for many potential applications such as nanoelectronics, sensors, batteries, supercapacitors, hydrogen storage and nanocomposites [1-5].

Among all the conducting polymers, polyaniline (Pani) is the most promising one. Because of its unique electrochemical properties such as simple reversible acid–base doping–dedoping chemistry, high electrical conductivity, good biocompatibility, ease of preparation, low cost

and good environmental stability, it has wonderful potential for commercial applications in electronic devices [6-12]. Recently, conducting polymer/ inorganic nanoparticles composites have found large number of applications like solar cells [13-15], anti-corrosion coatings, chemical sensors, memory devices, batteries, light emitting diodes, fuel cells, capacitors [7], electrochromic devices [16-18], gas sensors [19], conductive packaging [20-22] etc.

Well known surfactant, dodecylbenzenesulfonic acid (DBSA), forms colloidal solution and acts as a steric stabilizer. It disperses finely in an aqueous medium. The anilinium:DBSA suspension can be achieved through solution mixing. Due to the network structure of GN, aniline monomers adsorbed on the surface [23-25]. In addition, functional protonic acids such as DBSA can increase solubility of monomer molecules in organic solvents [26-27]. The long aliphatic chains of DBSA facilitate the conventional mixing of Pani:DBSA complexes

In this work, successful preparation of conducting and thermally stable Pani@GN nanocomposites by *in-situ* oxidative polymerization technique using surfactant dodecylbenzenesulfonicacid (DBSA) and cetyltrimethylammonium bromide (CTAB) is reported. Both the DBSA and CTAB caused uniform dispersion of graphene sheets within the polymer matrix besides DBSA acted as dopant also. Electrical conductivity and thermal stability depend on the amount of graphene nanofiller in the nanocomposites. Pani@GN:DBSA nanocomposites showed higher thermal stability and electrical conductivity than the Pani:DBSA. The structure, morphology and thermal stability of nanocomposites were also investigated. Study of DC electrical conductivity retention under isothermal and cyclic conditions are very important for assessing its potentiality for its use in various electrical and electronic devices such as charge storage devices. TGA and DSC ware used for the study of thermal properties of PANI:DBSA and Pani@GN:DBSA nanocomposites.

2. EXPERIMENTAL

2.1. Materials and chemicals

Aniline from E-Merck India Ltd. was purified by distilling twice before use and graphene (GN) used in this study was purchased from Iljin Nano Tech, Seoul, Korea. Dodecylbenzenesulfonicacid (DBSA) was purchased from Himedia Laboratories Pvt. Ltd., Mumbai, India. LR grade N-cetyl-N,N,N-trimethylammonium bromide (CTAB), potassium persulphate (PPS), HCl (AR grade) and methanol were purchased from CDH India Ltd. and used as received. The water used in all experiments was double distilled.

2.2. Preparation of Pani and Pani@GN nanocomposites

The nanocomposites of Pani@GN were prepared in the presence of CTAB by *in-situ* oxidative polymerization of aniline in the presence of different amounts of GN using potassium persulphate as an oxidizing agent. Required amount of GN nanoparticles **(Table 1)** was ultrasonicated for 2 h before pouring into the aniline solution. Polymerization was effected by the addition of potassium persulphate solution. The molar ratio of aniline:CTAB:oxidant was kept 1:1:0.5 in all the experiments. The resultant mixture was kept under continuous stirring for 20 h which later turned into greenish black slurry and was filtered. Thus prepared materials were washed thoroughly with double distilled water followed by methanol to remove excess of acid, potassium persulphate and polyaniline oligomers until filtrate became colorless and neutral. The nanocomposites containing different amounts of GN nanoparticles were dedoped by treating with 500 ml of 1M aqueous ammonia solution. Pani was also prepared using the same method as described above without the incorporation of GN. The technique used in this experiment is already reported elsewhere [28].

Pani and Pani@GN nanocomposites were redoped with 1M DBSA solution for over night under stirring then filtered, washed with distilled water and dried at 70-80^{o}C for 20 h in an air oven. The materials were converted into fine powders and were stored in desiccator for further investigations. Pani was also redoped using the same method as described above. Different samples were assigned different I.Ds as evident from **Table 1.** The preparation of pellets from fine powder of DBSA doped Pani and Pani@GN nanocomposites was done by using a hydraulic press under 37KN pressure for 10 minutes. Pellets were stored in desiccator for further studies.

Table 1. Preparation details of Pani and Pani@GN nanocomposites.

Sample I.D.	Volume of Aniline (mL)	Weight of $K_2S_2O_8$ (g)	Weight of DBSA Surfactant (g)	Weight of CTAB (g)	Weight of GN (g)
Pani:DBSA	10	15.0	19.0	40.0	0.00
Pani@GN:DBSA-1	10	15.0	19.0	40.0	0.1
Pani@GN:DBSA-2	10	15.0	19.0	40.0	0.2
Pani@GN:DBSA-3	10	15.0	19.0	40.0	0.3

3. CHARACTERIZATION

The Fourier transform infra-red spectroscopy (FTIR) spectra were recorded using Perkin Elmer 1725 spectrophotometer on KBr discs between 400 cm^{-1} and 4000 cm^{-1}. To study the surface morphology of Pani:DBSA and Pani@GN:DBSA nanocomposites, field emission scanning electron microscopy (FE-SEM) was done by LEO 435–VF. Samples were gold coated before imaging. The phase composition of Pani:DBSA and Pani@GN:DBSA nanocomposites were analyzed for XRD patterns recorded by Bruker D8 diffractometer with Cu Kα radiation at 1.540 Å in the range of $50^0 \leq 2\theta \leq 70^0$ at 40 kV. The thermogravimetric analysis (TGA) was performed on the selected samples of Pani:DBSA and Pani@GN:DBSA nanocomposites by Perkin Elmer (Pyris Dimond) instrument from ~25°C to ~800°C at the heating rate of 10°C min^{-1} at the nitrogen flow rate of 200 ml^{-min} and DTA was done by automatic thermal analyzer (V2.2A Du Pont 9900). The measurements of DC electrical conductivity (σ) retention under isothermal and cyclic ageing conditions of Pani:DBSA and Pani@GN:DBSA nanocomposites ware also done. In the isothermal stability testing, the pellets were heated at 50, 70, 90, 110 and 130°C in an air oven. The DC electrical conductivity was measured at an interval of 10 min. in the accelerated ageing experiments. While in the cyclic ageing technique, DC electrical conductivity measurements were taken 5 times at an interval of about 45 min. within the temperature range of 40-150°C. An instrument with four-in-line probe with a temperature controller, PID-200 (Scientific Equipments, Roorkee, India) was used for DC electrical conductivity measurements and its temperature dependence. The DC electrical conductivity was calculated by using the following equation:

$$\sigma=[\ln 2(2S/W)]/[2\pi S(V/I)] \quad \textbf{Equation (1)}$$

Where I, V, W and S are the current (A), voltage (V), thickness of the film (cm) and probe spacing (cm) respectively and σ is the conductivity (Scm^{-1}) [29].

4. RESULTS AND DISCUSSION

4.1. Synthesis of Pani:DBSA and Pani@GN:DBSA nanocomposites

Pani:DBSA and Pan@GN:DBSA nanocomposites have been synthesized via *in-situ* oxidative polymerization technique containing different amount of GN. DBSA used in the synthesis not only dispersed GN uniformly, but it also acted as dopant. Pani synthesis in the presence of anionic surfactants, such as DBSA which forms micelle provides a template for the synthesis of high molecular weight Pani with good electrical properties and stability. The doping of Pani with DBSA is similar to when Pani is doped with any other inorganic acid. The protons of the DBSA interact with imine nitrogens resulting into the formation of holes on Pani backbone leading to the increase in electrical conductivity [30, 31].

4.2. Fourier transform infra-red (FTIR) spectroscopic studies

The FTIR spectra of graphene, Pani:DBSA and Pani@GN:DBSA-2 are shown in **Figure 1**. The characteristic peaks of Pani:DBSA occur at 3390, 3242, 2924, 3052, 1588, 1497, 1306, 1143, 1035 and 831, 691 and 615 cm^{-1}.The peak at 3390 cm^{-1} may be attributed to the free N–H (non-hydrogen bonded) stretching vibration [332]. The weak shoulders at 2924-3052 cm^{-1}

correspond to aromatic sp^2 CH stretching [33]. The bands at 1588 cm^{-1} and 1497 cm^{-1} are due to stretching mode of the quinoid and stretching mode of benzenoid rings respectively [34] and the peak at about 1306 cm^{-1} can be related to the C–N stretching mode of secondary aromatic amine [35]. The peak at 831 cm^{-1} is usually assigned to an out-of-plane bending vibration of C−H of 1, 4-disubstituted benzenoid rings which confirms the formation of Pani [36]. The presence of DBSA has been confirmed by the peaks at 1143 and 691 cm^{-1} corresponding to the O=S=O and S-O stretching vibrations respectively [37].

The FTIR spectrum of Pani@GN:DBSA-2 is identical to that of Pani:DBSA but some of the peaks of Pani@GN:DBSA have shifted from their positions and no new peaks have emerged in the spectrum of nanocomposite. Therefore, it may be inferred that the incorporation of GN does not alter the backbone structure of Pani.

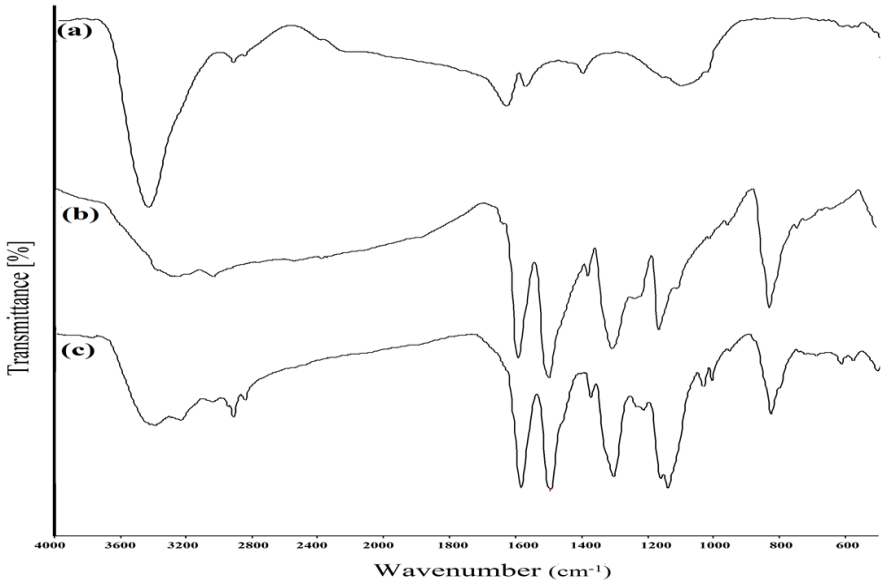

Figure 1 FTIR spectra of: (a) graphene (b) Pani:DBSA (c) Pani@GN:DBSA-2

4.3. Field emission scanning electron microscopic (FESEM) studies

The morphology of undoped Pani and Pani:DBSA and Pani@GN:DBSA-2 were studied by FESEM as shown in **Figure 2.** The fine granular and tubular structures may be observed in case of Pani. In case of the Pani:DBSA-2, it shows irregular morphology with rod like shape of DBSA coated Pani. In case of Pani@GN:DBSA-2, it shows uniform coating of Pani on the surface of GN. This indicates that GN supports the uniform adsorption of aniline monomer on its surface due to the electrostatic interaction. When PPS was added into the reaction mixture of GN and aniline, the adsorbed aniline molecules underwent polymerization on the adsorbed sites and started growing resulting to the formation of the agglomerated, lamellar and rod like structures [38]. It is understood that some aniline monomer may have polymerized on the surface of GN templates and the remaining aniline monomer may have polymerized into granular and tubular structures.

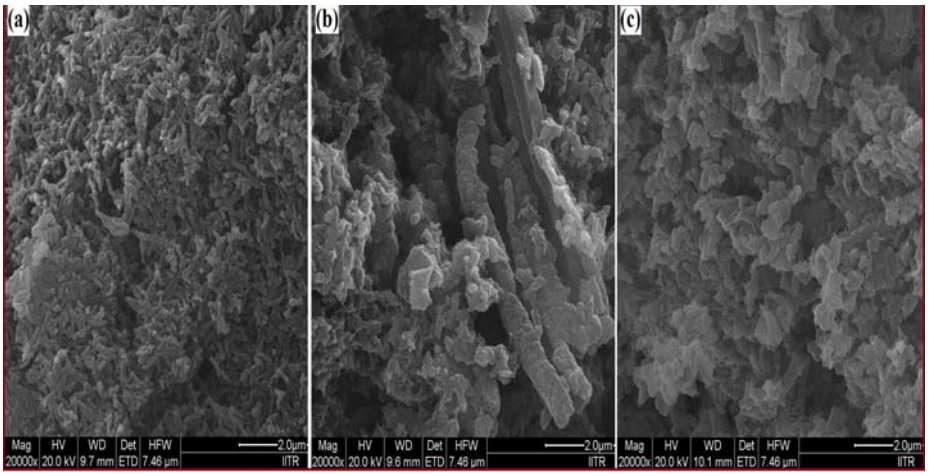

Figure 2 FE-SEM images of: (a) Pani, (b) Pani:DBSA and (c) Pani@GN:DBSA-2

4.4. X-ray diffraction (XRD) Studies

Figure 3. Shows the XRD Patterns of Pani:DBSA and Pani@GN:DBSA-2. The XRD pattern of Pani:DBSA showed a single broad peak at 2θ = 17°-24.8° which may be attributed to the periodicity parallel to the polymer chain indicative of amorphous nature of Pani [39]. The presence of sharp peaks at higher 2θ = 37˚, 43.4˚, 63.8˚ and 76.9˚ may correspond to the higher degree of crystalline nature of the material [40, 41]. The XRD pattern of Pani@GN:DBSA-2 shows the increase in the intensity of peak, while the peak at 2θ = 25.8° supports presence of GN in the Pani:DBSA. This peak suggests d-spacing between graphene layers (0.33 nm) [42] and better dispersion of GN in the Pani:DBSA inducing more regular order and hence an increase in the crystallinity.

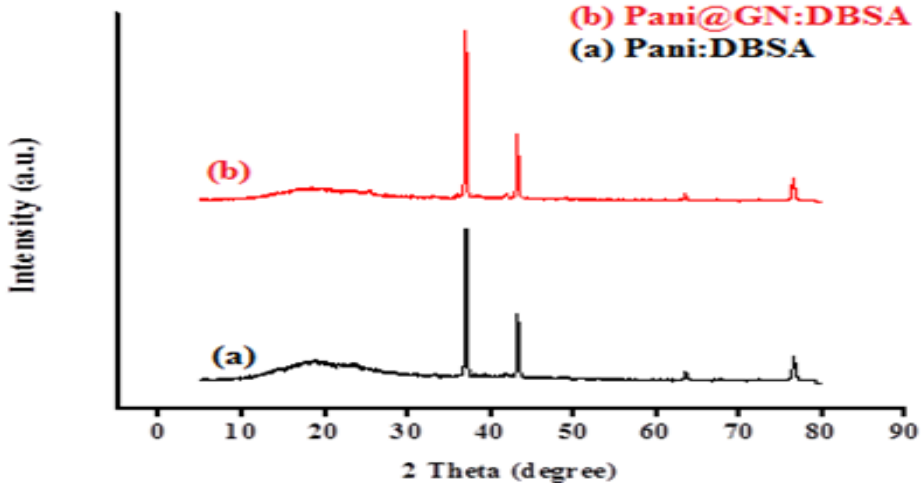

Figure 3 XRD spectra of: (a) Pani:DBSA and (b) Pani@GN:DBSA-2

4.5. Thermogravimetric analysis (TGA) studies

Thermogravimetric analysis (TGA) was used to examine the thermal stability of Pani@GN:DBSA-2 as compared with Pani:DBSA. In the case of Pani:DBSA, **(Figure 4)** that there are two major stages of weight loss, the first weight loss till ~150°C is due to the loss of water and volatile solvent. The second weight loss occur from the temperature 290°C continues onward due to removal of dopant molecule and lower oligomers of Pani and followed by massive weight loss due to thermo-oxidative decomposition of Pani [43, 44]. When compared with the TGA of Pani@GN:DBSA-2, it may be observed that the degradation of nanocomposite is somewhat similar to that of Pani:DBSA. The noticeable difference is the thermal stability Pani@GN:DBSA-2, the major weight loss between temperature 390°C - 510°C may be due to some stabilizing interaction between Pani:DBSA and the GN.

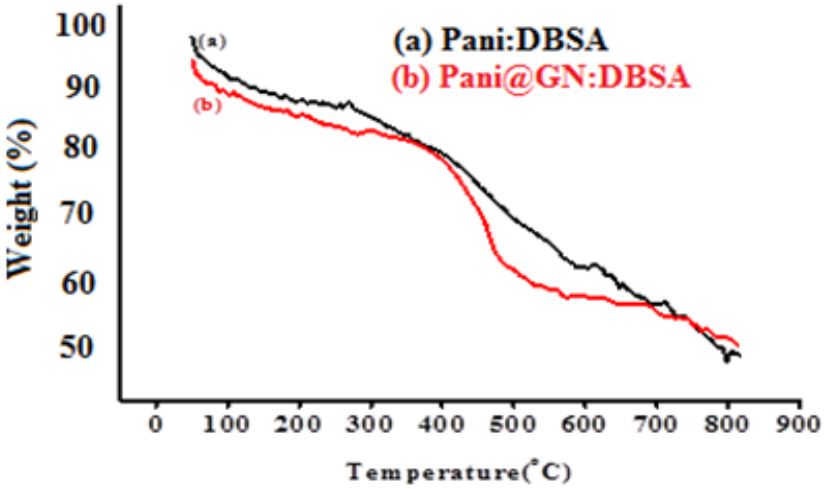

Figure 4 TGA of: (a) Pani:DBSA and (b) Pani@GN:DBSA-2

4.6. Differential thermal analysis (DTA) studies

Figure 5 show the DTA plots of Pani:DBSA and Pani@GN:DBSA-2. Both the samples show two endothermic peaks one at around 170–250°C and another at around 300–380°C. The first endothermic peak may be due to the loss of moisture and the second for the loss of dopant molecule and lower oligomers of Pani [45, 46]. The first peak is stronger in both the cases.

The result reflects that in presence of aromatic dopants bond formation of water molecules with the backbone nitrogen of the polymers is slightly similar when compared with those of Pani@GN:DBSA-2.

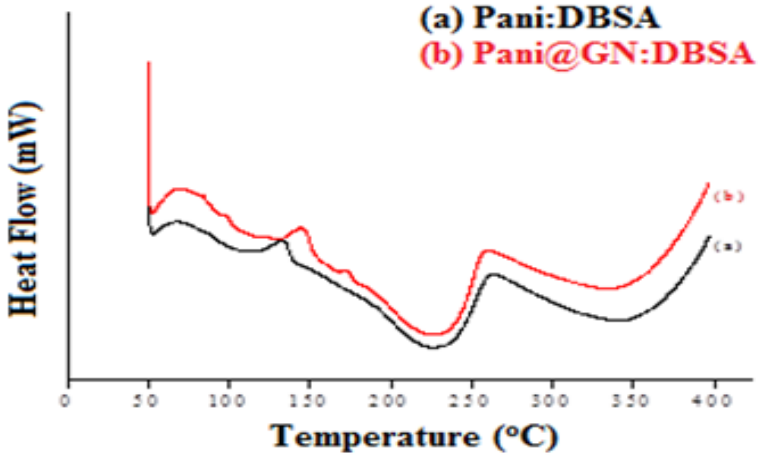

Figure 5 DTA of: (a) Pani:DBSA and (b) Pani@GN:DBSA-2

5. DC ELECTRICAL CONDUCTIVITY

The initial electrical conductivities of DBSA doped Pani and Pani@GN nanocomposites containing different amount of GN were measured by standard 4-in-line probe technique. From the electrical conductivity measured, it may be observed that all the samples are semiconducting in nature and the addition of GN nanosheets has significant effect on the conductivity. Electrical conductivity of Pani@GN nanocomposites is higher than that of Pani and it increased with increase in GN content in the nanocomposites. Since DBSA doped Pani as well as GN are good conducting in nature, hence the enhancement in DC electrical conductivity may be credited to the additive synergism of both the constituents interacting at molecular level. The increase in DC electrical conductivity with increase in GN content has been shown in **Figure 6.**

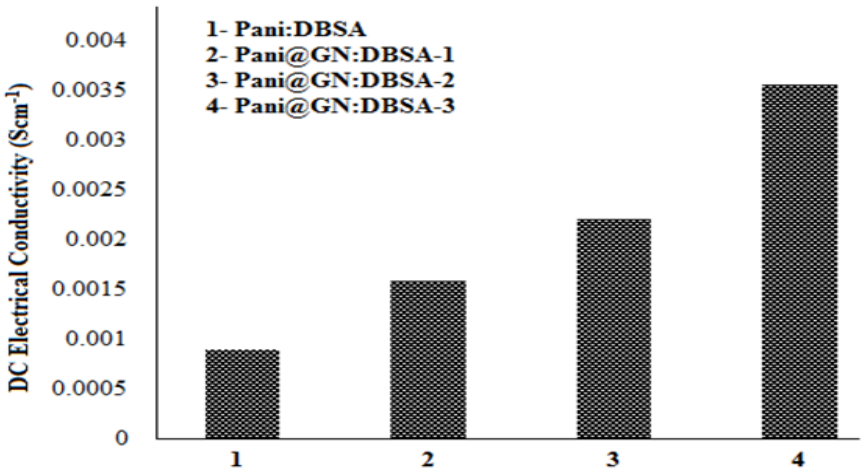

Figure 6 Initial DC electrical conductivities of DBSA doped Pani and Pani@GN nanocomposites

5.1. Mechanism of electronic conduction

This increment in electrical conductivity of Pani@GN nanocomposites can better be explained on the basis of band theory of conduction. In Pani, the extended π-electrons are present which are susceptible to undergo either oxidation or reduction. Here these π-electrons present on imine N-atom serve as valence band. On the other hand vacant, p_z orbital of C atoms present in GN serves as conduction band. When GN comes in contact with Pani, electrons from Pani jump to the vacant p_z orbitals of C atoms (responsible for electronic conduction). Thus movement of electrons becomes comparatively easier via electron-hole charge carriers resulting enhancement in electrical conductivity as shown in Scheme 1.

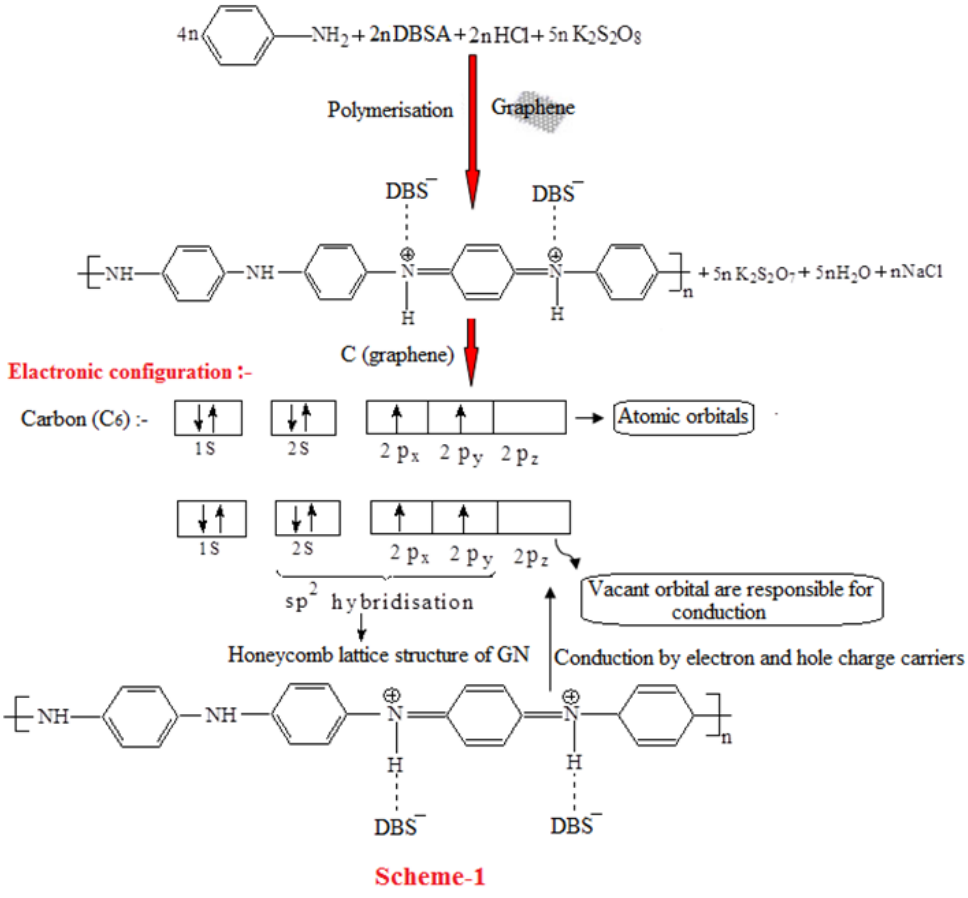

Scheme-1 Schematic representation of mechanism of electronic conduction

5.2. Isothermal stability studies

Under isothermal ageing conditions, the stability in terms of DC electrical conductivity retention of DBSA doped Pani and Pani@GN nanocomposites was studied **(Figure 7).** In order to evaluate the stability in terms of DC electrical conductivity of these nanocomposites, the relative electrical conductivity with respect to time at different temperatures for different samples was evaluated.

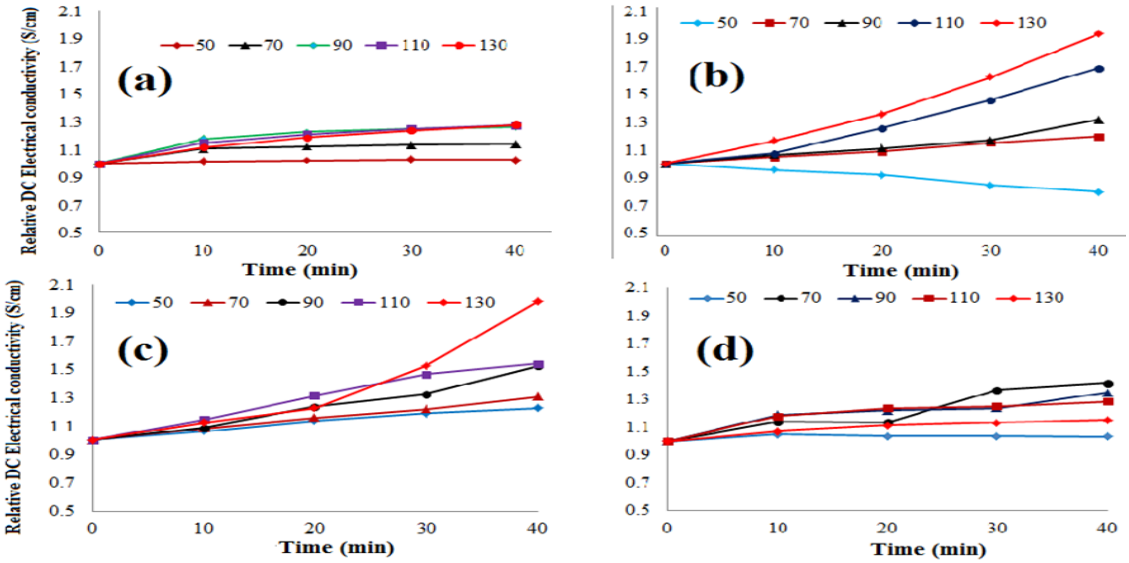

Figure 7 Relative electrical conductivity of: **(a)** Pani:DBSA, **(b)** Pani@GN:DBSA-l, **(c)** Pani@GN:DBSA-2 and **(d)** Pani@GN:DBSA-3 variation with time under isothermal ageing conditions

The DC conductivity of the samples (5 readings of each sample were taken at an interval of 10 min) was measured at the temperatures 50°C, 70°C, 90°C, 110°C and 130°C. The relative electrical conductivity was plotted against time for each temperature using the equation-2:

$$\sigma_{r,t} = \frac{\sigma_t}{\sigma_0} \qquad \text{Equation- 2}$$

where $\sigma_{r,t}$ = relative electrical conductivity at time t, σ_t = electrical conductivity at time t, σ_o = electrical conductivity at time zero.

Figure 7 (c & d) shows the relative electrical conductivity of Pani and all the nanocomposites fairly stable at all the temperatures.

In 50ºC, 70°C, 90°C, 110°C, 130°C except Pani@GN:DBSA-1 at 130ºC which shows lowering in it DC electrical conductivity over the period of the experiment.

5.3. Stability under cyclic ageing

The cyclic ageing technique within the temperature range of 40°C to 150°C was studied for DBSA doped Pani and Pani@GN nanocomposites in order to evaluate the stability in the terms of DC electrical conductivity **(Figure 8).** From the conductivity measurements, it was observed that the conductivity increased gradually from first to fifth cycle showing a regular trend in all the cases. The relative electrical conductivity was calculated using the following equation:

$$\sigma_r = \sigma_T / \sigma_{40} \qquad \textbf{Equation-3}$$

where, σ_r is relative electrical conductivity, σ_T is electrical conductivity at temperature T (°C) and σ_{40} is electrical conductivity at 40°C.

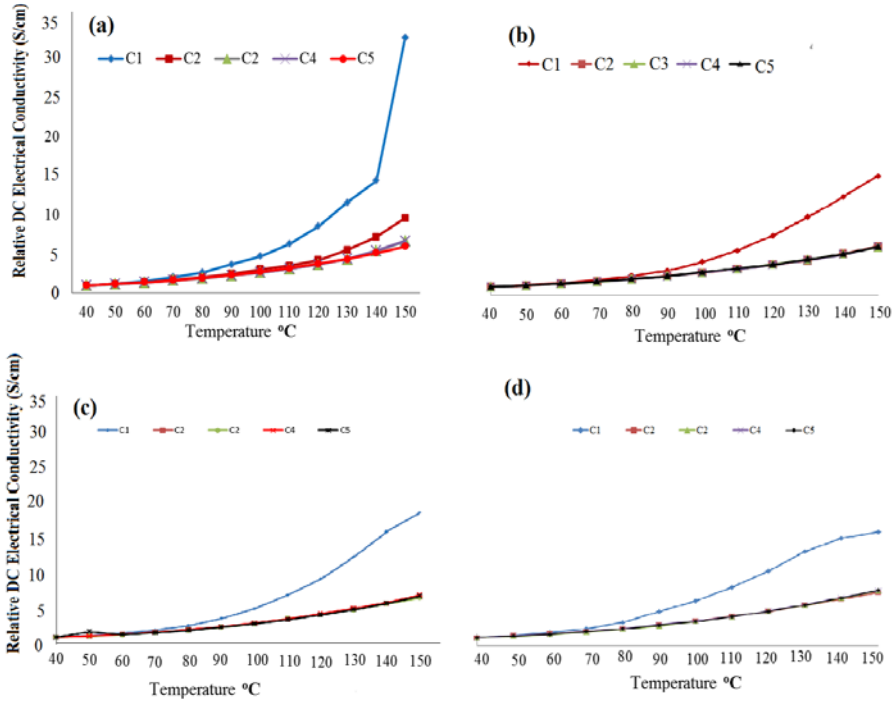

Figure 8 Relative electrical conductivity of **(a)** Pani:DBSA, **(b)** Pani@GN:DBSA-l, **(c)** Pani@GN:DBSA-2 and **(d)** Pani@GN:DBSA-3 under cyclic ageing conditions.

The DC electrical conductivity of Pani and all the Pani@GN nanocomposites showed good stability upto 150°C when cycled in the temperature range of 40-150°C (**Figure 8**). Thus it may be noted that the nanocomposites became stable semiconductors after first cycle. This may be attributed to the removal of moisture and annealing in the first cycle leading to stabilization. Thus, it may be suggested that preliminary annealing at ~80°C could be done for stabilization of the nanocomposites.

6. CONCLUSIONS

The results of this study suggest that we have successfully prepared Pani and Pani@GN nanocomposites by simple *in-situ* oxidative polymerization method in presence of CTAB where DBSA was used as redoping agent. The characterization and stability in terms of DC electrical conductivity retention under isothermal and cyclic ageing conditions have also been presented. The results of this study suggest that the incorporation of DBSA into Pani as well as in Pani@GN nanocomposites cause significant increase in the electrical conductivity and its stability.

The others, as prepared Pani@GN nanocomposites were observed to possess higher electrical conductivity and better isothermal as well as cyclic stability in terms of electrical conductivity retention than that of Pani. This increment may be attributed to the addition of ultrasonicated GN nanosheets in the polymer matrix and may be postulated as a universal approach to prepare nanocomposites with enhanced electrical conductivity. Thus, as prepared Pani@GN nanocomposites may find better realistic applications in modern electronic devices compared with Pani and seems to be a replaceable alternate even for metals in the next generation devices.

ACKNOWLEDGEMENTS

One of the authors (Mahfoozurrahman Khan) is thankful to Dr. Mohd Omaish Ansari for their suggestions.

REFERENCES

[1] Kim KS, Zhao Y, Jang H, Lee SY, Kim JM, Kim KS, Ahn JH, Kim P, Choi JY, Hong BH. 2009. Large-scale pattern growth of graphene films for stretchable transparent electrodes. Nature 457:706-710.

[2] Geim AK, Novoselov KS. 2007. The rise of graphene. Nat Mater 6:183–191.

[3] Kopelevich Y, Esquinazi P. 2007. Graphene Physics in Graphite. Adv Mater 19:4559-4563.

[4] Lee DH, Kim JE, Han TH, Hwang JW,

Jeon S, Choi SY et al. 2010. Versatile carbon hybrid films composed of vertical carbon nanotubes crown on mechanically compliant graphene films. Adv Mater 22:1247–1252.

[6] Stejskal J. 2002. Polyaniline preparation of a conducting polymer. Pure Appl Chem 74: 857-867.

[7] MacDiarmid AG. 2001. Synthetic metals: A novel role for organic polymers (Nobel lecture). Angew Chem Int Ed 40:2581–2590.

[8] Thiyagarajan M, Kumar J, Samuelson LA, Cholli AL. 2003. Enzymatically synthesized conducting polyaniline nanocomposites: A solid state NMR study. J Macromol Sci A 40:1347-13455.

[9] Wu M, Zhang L, Wang D, Gao J, Zhang S. 2007. Electrochemical capacitance of MWCNT/polyaniline composite coatings grown in acidic MWCNT suspensions by microwave-assisted hydrothermal digestion. Nanotechnology 18: 385603.

[10] Yang CY, Cao Y, Smith P, Heeger AJ. 1993. Morphology of conductive, solution
Processed blends of polyaniline and poly(methyl methacrylate). Synth Met 53:
293-301.

[11] Ikkala OT, Laakso J, Vakiparta K, Virtanen E, Ruohonen H, Jarvinen H et al. 1995. Counter-ion induced processibility of polyaniline: Conducting melt processible polymer blends. Synth Met 69:97-100.

[12] Tiitu M, Talo A, Forsén O, Ikkala O. 2005. Aminic epoxy resin hardeners as reactive solvents for conjugated polymers: Polyaniline base/epoxy composites for anticorrosion coatings. Polymer 46:6855-6861.

[13] Sailor MJ, Curtis CL. 1994. Conductiong polymer connections for molecular devices. Adv Mater 6:688-692.

[14] Ameen S, Akhtar MS, Kim YS, Yang OB, Shin HS. 2011, An effective nanocomposite of polyaniline and ZnO: Preparation, characterizations, and its photocatalytic activity. Colloid Polym Sci 289:415-421.

[15] Wright M, Uddin A. 2012. Organic-inorganic hybrid solar cells: A comparative review. Sol Energy Mater Sol Cells 107:87-111.

[16] Kim D Y, Kim J, Kim J, Kim A, Lee G, Kang M. 2012. The photovoltaic efficiencies on dye sensitized solar cells assembled with nanoporous carbon / TiO_2 composites. J Ind Eng Chem 18:1-5.

[17] Bai H, Shi G. 2007. Gas Sensors Based on Conducting Polymers. Sensors 7:267-307.

[18] Bae J, Jang J. 2012. Fabrication of carbon nanotubes from conducting polymer precursor as field emitter. J Ind Eng Chem 18:1921-1924.

[19] Virji S, Huang J, Kaner RB, Weiller BH. 2004. Polyaniline nanofiber gas sensors: examination of response mechanisms. Nano Lett 4:491-496.

[20] Youssef A M, El-Samahy M A, Abdel Rehim M H. 2012. Preparation of conductive paper composites based on natural cellulosic fibers for packaging applications. Carbohydr Polym 89:1027-1032.

[21] Youssef AM, Kamel S, El-Sakhawy M, El Samahy MA. 2012. Structural and electrical properties of paper-polyaniline composite. Carbohydr Polym 90:1003-1007.

[22] Reddy KR, Sin BC, Ryu KS, Noh J, Lee Y. 2009. In situ self-organization of carbon black-polyaniline composites from nanospheres to nanorods: Synthesis, morphology, structure and electrical conductivity. Synth Met 159:1934-1939.

[23] Kohut-Svelko N, Reynaud S, François J. 2005. Synthesis and characterization of polyaniline prepared in the presence of nonionic surfactants in an aqueous dispersion. Synth Met 150:107-114.

[24] Kim S, Ko JM, Chung IJ. 1996. Electrical conductivity change ofpolyaniline–dodecyl benzene sulfonic acid complex with temperature. Polym Adv Technol 7:599–603.

[25] Jia W, Segal E, Kornemandel D, Lamhot Y, Narkis M, Siegmann A. 2002. Polyaniline-DBSA/organophilic clay nanocomposites : synthesis and characterization. System 128:1-6.

[26] Cao Y, Smith P, Heeger AJ. 1992. Counter-ion induced processibility of

conducting polyaniline and of conducting polyblends of polyaniline in bulk polymers. Synth Met 48: 91-97.

[27] Guo H, Zhu H, Lin H, Zhang J. 2008. Synthesis of polyaniline/multi-walled carbon nanotube nanocomposites in water/oil microemulsion. Mater Lett 62:3919-3921.

[28] Anwer T, Ansari MO, Mohammad F. 2013. Morphology and thermal stability of electrically conducting nanocomposites prepared by sulfosalicylic acid micelles assisted polymerization of aniline in presence of ZrO_2 nanoparticles. Polym Plast Technol Eng 52:472-477.

[29] Ansari MO, Mohammad F. 2011. Thermal stability, electrical conductivity and ammonia sensing studies on p-toluenesulfonic acid doped polyaniline:titanium dioxide (pTSA/Pani:TiO_2) nanocomposites. Sensors Actuators, B Chem 157:122–129.

[30] Xu J, Yao P, Liu L, Jiang Z, He F, Li M, Zou J. 2010. Synthesis and characterization of an organic soluble and conducting polyaniline-grafted multiwalled carbon nanotube core-shell nanocomposites by emulsion polymerization. J Appl Polym Sci 118: 2582-2591

[31] Yao P, Xu J, Wang Y, Zhu C. 2009. Preparation and characterization of soluble and DBSA doped polyaniline grafted multi-walled carbon nanotubes nano-composite. J Mater Sci Mater Electron 20: 891-898.

[32] Qiang J, Yu Z, Wu H, Yun D. 2008. Polyaniline nanofibers synthesized by rapid mixing polymerization. Synth Met 158: 544-547.

[33] Yan XB, Han ZJ, Yang Y, Tay BK. 2007. NO_2 gas sensing with polyaniline nanofibers synthesized by a facile aqueous/organic interfacial polymerization. Sensors Actuators, B Chem 123:107-113.

[34] Tiwari A, Kumar R, Prabaharan M, Pandey RR, Kumari P, Chaturvedi A et al. 2010. Nanofibrous polyaniline thin film prepared by plasma-induced polymerization technique for detection of NO_2 gas. Polym Adv Technol 21:615-620.

[35] Cruz-Silva R, Romero-Garcia J, Angulo-Sánchez J L, Flores-Loyola E, Farias M H, Castillon FF et al. 2004. Comparative study of polyaniline cast films prepared from enzymatically and chemically synthesized polyaniline. Polymer 45:4711-4717.

[36] Mallick K, Witcomb MJ, Scurrell MS. 2007.Directional assembly of polyaniline functionalized gold nanoparticles. J Phys Condens Matter 19:196225.

[37] Anilkumar P, Jayakannan M. 2007. Fluorescent tagged probing agent and structure-directing amphiphilic molecular design for polyaniline nanomaterials via self-assembly process. J Phys Chem C 111:3591-3600.

[38] Li J, Xie H, Li Y, Liu J, Li Z. 2011. Electrochemical properties of graphene nanosheets/polyaniline nanofibers composites as electrode for supercapacitors. J Power Sources 196:10775-10781.

[39] Saravanan S, Joseph Mathai C, Anantharaman M R, Venkatachalam S, Prabhakaran P V. 2006. Investigations on the electrical and structural properties of polyaniline doped with camphor sulphonic acid. J Phys Chem Solids 67:1496-1501.

[40] Gupta K, Chakraborty G, Ghatak S, Jana PC, Meikap A K, Babu R. 2010. Synthesis, magnetic, optical, and electrical transport properties of the nanocomposites of polyaniline with some rare earth chlorides. J Appl Phys 108. doi:10.1063/1.3489899.

[41] Stejskal J. 2002. Polyaniline. preparation of a conducting polymer. Pure Appl Chem 74: 857-867.

[42] Tung NT, Van Khai T, Jeon M, Lee YJ, Chung H, Bang J H et al. 2011. Preparation and characterization of nanocomposite based on polyaniline and graphene nanosheets. Macromol Res 19:203-208.

[43] Deng J, He CL, Peng Y, Wang J, Long X, Li P, Chan ASC. 2003. Magnetic and Conductive Fe_3O_4–polyaniline nanoparticles with core–shell structure Synth Met 139:295-301.

[44] He Y. 2004. Preparation of polyaniline/nano-ZnO composites via a novel pickering emulsion route. Powder Technol 147:59–63.

[45] Bhadra S, Khastgir D. 2008. Extrinsic and intrinsic structural change during heat treatment of polyaniline. Polym Degrad Stab 93:1094-1099.

[46] Bhadra S, Khastgir D. 2007. Degradation and stability of polyaniline on exposure to electron beam irradiation (structure-property relationship). Polym Degrad Stab 92:1824-1832.